Bearingless Reluctance Slice Motors

Wolfgang Gruber*
ACCM GmbH (JKU Linz)
Linz, Austria

Wolfgang Briewasser
ACCM GmbH (JKU Linz)
Linz, Austria

Michael Rothböck
ACCM GmbH (JKU Linz)
Linz, Austria

Reto T. Schöb
Levitronix GmbH
Zurich, Switzerland

Wolfgang Amrhein
ACCM GmbH (JKU Linz)
Linz, Austria

Abstract

Bearingless permanent magnet motors are very compact and favorable for high speed designs. Especially the bearingless slice motor (using a permanent magnet excited rotor disc) features a mechanically simple and very cost effective fully magnetically levitated system by stabilizing some degrees of freedom by permanent magnetic reluctance forces.

This work focuses on constructional possibilities to apply the slice rotor principle with its passive stabilization without any permanent magnets in the rotor part. As a matter of fact, the permanent magnets are necessary and are therefore located in the stator. Possible stator compositions are outlined and separated into homopolar and heteropolar permanent magnet air gap flux types. The definition of performance parameters allows evaluating the operational behavior of the two considered bearingless reluctance slice motor types (one with hompolar and one with heteropolar air gap flux distribution).

The composition, optimization and construction of a prototype are outlined in the last section. Measurements are conducted to show the proper functionality of the bearingless reluctance slice motor prototype.

1 Introduction

During the last few years a lot of research has been done to work out different concepts for bearingless drives and bearingless motors in particular [1]. Bearingless motors are capable of creating radial bearing forces and drive torque with one common lamination stack. Therefore, very compact magnetically suspended systems can be designed that are well suited for high speed operation [2], [3] and for high purity environments by hermetically sealing the rotor from the stator [4]. To reduce system complexity, a very simple mechanical design can be achieved using bearingless slice motors, where the axial position and tilting effects are passively stabilized by permanent magnetic reluctance forces [5]. The permanent magnets that produce the air gap field (necessary for stabilization, bearing forces and motor torque) are normally located on or in the rotor [6], [7].

However, in some applications the rotor is a disposable (e. g. in medical blood pumps) or can become very hot. For this reason permanent rotor magnets are unfavorable due to their high price and temperature limitations. Thus, in this work bearingless slice motors without any magnetic material in the rotor are studied, leading instantly to bearingless reluctance motors, which are biased from stator permanent magnets, to create the passive reluctance forces for the stabilization of some degrees of freedom.

Bearingless reluctance motors are well known in literature [8]-[10]. They are reported to possess inherent advantageous features such as fail safe, robustness, low cost and possible operation in high temperatures or in intense temperature variations. Torque is produced by magnetic attraction of rotor and stator poles, and a significant amount of radial force can be produced in the process.

There are also reluctance rotor drive systems with conventional mechanical bearings, featuring permanent magnets in the stator. They are called alternate flux-switching or (hybrid excitation) doubly salient (permanent magnet) machines [11]. They are of interest due to their simple and robust rotor design and their high torque density. However, up to now no bearingless reluctance slice motor design was reported in literature.

*Contact Author Information: E-mail: wolfgang.gruber@jku.at
Address: Johannes Kepler University Linz, Altenberger Str. 69, A-4040 Linz
Phone: +43-732-2468-6435
Fax: +43-732-2468-6423

2 Constructional Examples

This section deals with possible design variants for bearingless reluctance slice motors. Whereas there is only a small variety in rotor designs, the composition of the stator can be manifold.

2.1 Reluctance Rotor Variants

The rotor topology for bearingless slice reluctance motor relates to the rotor of common switched or synchronous reluctance drives. Basically there are only two different rotor types. The left cross section in Fig. 1 shows a rotor that features flux barriers to create the saliency. The outer surface of the rotor can be circular in this case. The rotor depicted on the right-hand side features an alternating air gap to create the rotor angle dependant reluctance which is needed for torque generation.

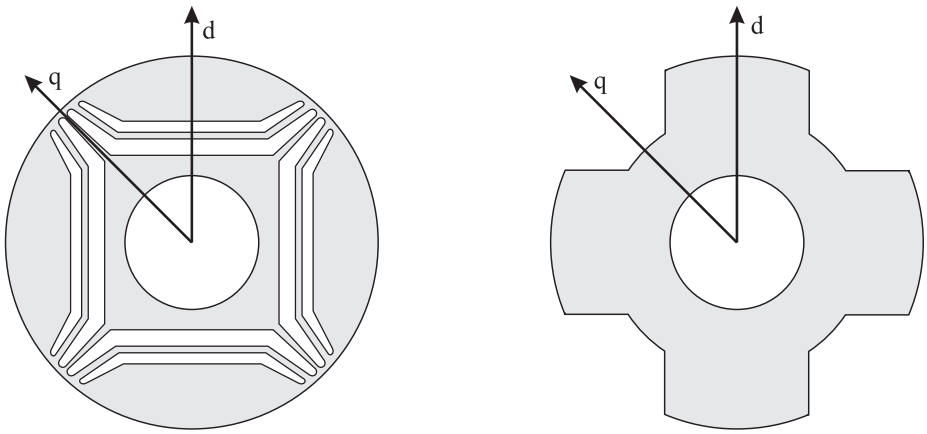

Figure 1: Common reluctance rotor topologies, featuring four pole pairs

2.1 Stator Variants

In contrast to the classical approach, bearingless slice reluctance motors must incorporate the permanent magnets in the stator and not in the rotor. In this case the permanent magnet air gap bias flux density might be unipolar or bipolar around the circumference. The following sections discuss different stator design variants.

2.4.1 Heteropolar air gap flux distribution

Stator compositions that possess alternating permanent magnet bias flux distributions in the air gaps are referred as heteropolar bearingless reluctance slice motors. Figure 2 and 3 show possible variants of this kind of bearingless reluctance slice motor. The permanent magnetic flux lines close in two dimensional planes normal to the motor axis.

Referring to common electrical drives, the right cross section in Fig. 2 is called alternate flux-switching drive. In this drive the permanent magnets are buried in the stator, whereas on the left-hand side the stator permanent magnets are surface mounted. Both cross sections feature four stator teeth, each holding a concentrated winding. The permanent magnets create two alternating magnetic poles on each stator tooth. An excitation of a coil will strengthen one permanent magnetic pole, while simultaneously weakening the other magnetic pole of the stator tooth. This leads to a rotor angle dependent generation of radial bearing forces and motor torque. It is also obvious that the permanent magnetic induced voltage in the stator coils are varied by the rotor angle dependant reluctance.

Alternative stator setups are visualized in Fig. 3. These motor cross sections are often referred to as doubly salient permanent magnet machines. In the depicted cross sections, the stators feature concentric coils wound around one stator tooth. In contrast to the previous designs in Fig. 2, there exists only one magnetic pole per stator tooth. With reference to first finite element investigations, these motors do possess strong reluctance forces due to the stator currents and are therefore hard to control. There are some further possible types of heteropolar bearingless reluctance slice motors. Some of these can be found in [12].

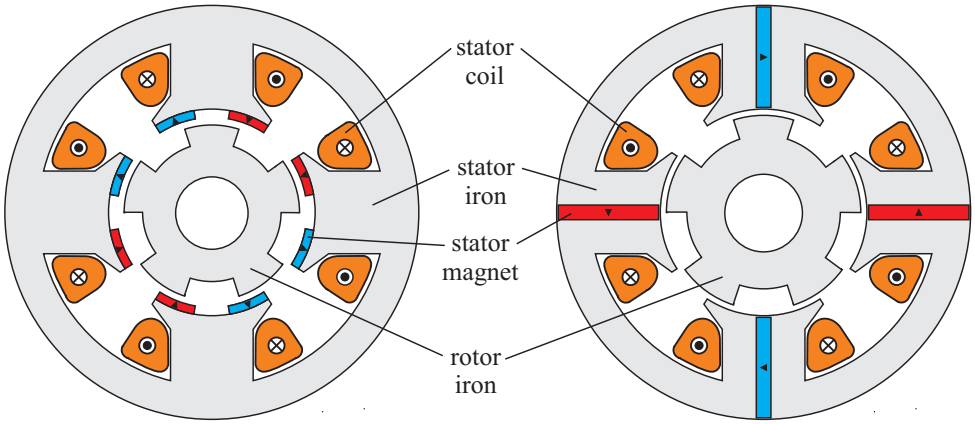

Figure 2: Cross sections of two heteropolar bearingless reluctance slice motor variants.
The permanent magnets create two opposing poles on each stator tooth.

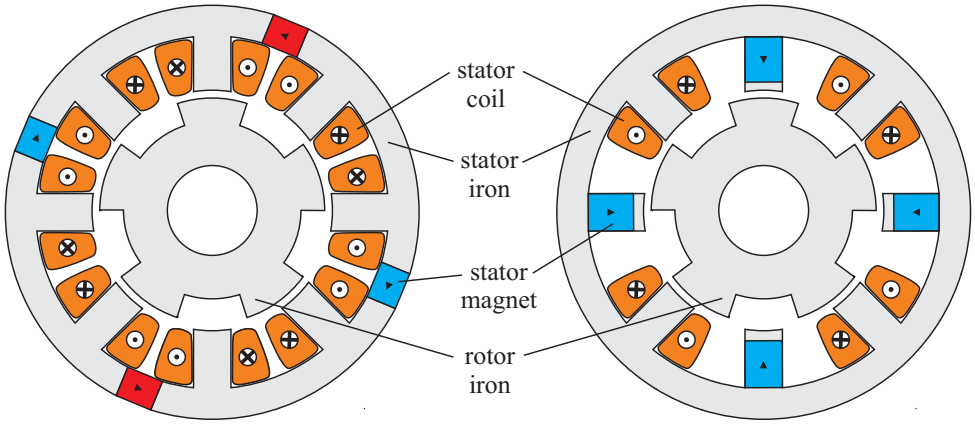

Figure 3: Cross sections of two heteropolar bearingless reluctance slice motors.
Each stator tooth features one permanent magnetic pole.

2.4.1 Homopolar air gap flux distribution

In order to reduce iron losses especially at very high speeds, a homopolar magnetic bias flux is often used in active magnetic bearings. Such a flux distribution can also be achieved in bearingless reluctance slice motors. Figure 4 shows two different examples. In contrast to heteropolarly biased motors, a three dimensional flux distribution mostly along radial and axial direction becomes necessary. The homopolar bearingless reluctance slice motor features two air gaps, an outer and an inner gap between rotor and stator. The flux lines penetrate the rotor from the outer air gap and leave the rotor by the inner air gap. Thus, the outer and inner air gap features a homopolar flux distribution. Both air gap fields create stabilizing reluctance forces in axial and tilting direction. A sealing of the rotor into a tight hermetic chamber might be more difficult compared to the heteropolar designs due the two air gaps.

The left design in Fig. 4 is a so-called temple motor. The stator teeth are bent in axial direction and the stator coils are wound around these axial parts. An axially magnetized permanent magnet cylinder in the centre creates the bias flux in the air gaps. A cover plate on top of the magnet leads the flux from the stator into the rotor part.

An axially more compact homopolar bearingless slice motor design variant is depicted on the right side of Fig. 4. The coils are placed on the stator teeth in radial direction. In contrast to the temple motor design, the electromagnetic coil flux is kept within planes normal to the motor axis. The bias flux is created by an axially magnetized permanent magnet ring on the stator's outer side.

The basic magnetic characteristics as well as the force and torque generation capability are quite equal for both illustrated concepts.

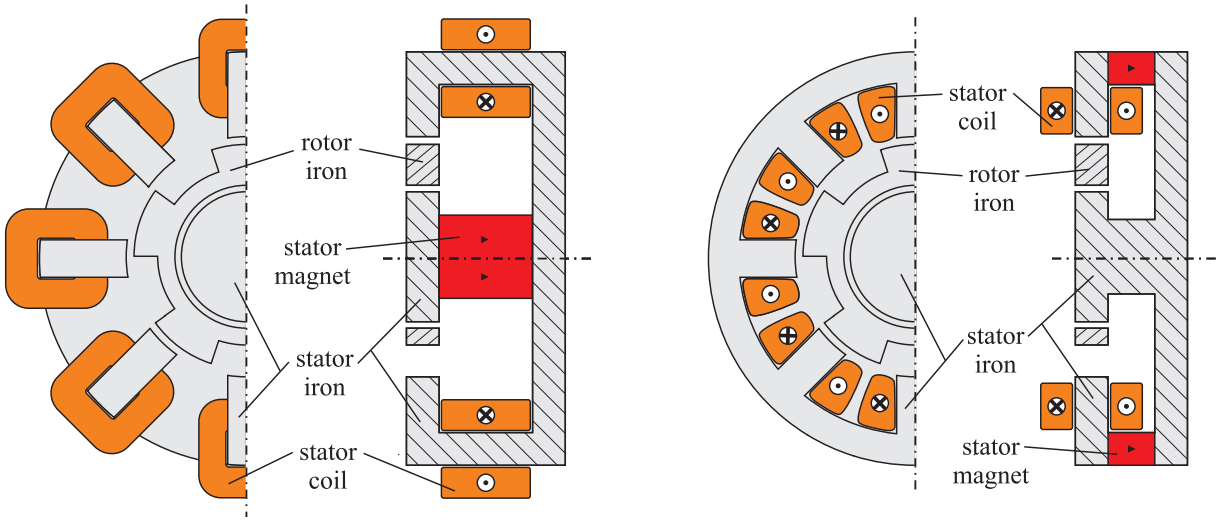

Figure 4: Composition of two different homopolar bearingless reluctance slice motor designs.

3 Control of the Bearingless Slice Motor

This section focuses on the theoretical background of the combined force and torque generation by one common winding system in bearingless slice motors. At first, the mathematical model is derived. The separation of bearing forces and motor torque by a proper excitation of the coils is outlined. Finally, performance parameters are defined.

3.1 Force and Torque Generation

It is known from [13], that by the help of the Maxwell stress tensor for any motor in centered rotor position the resulting radial forces F_x and F_y together with the motor torque T_z can be described generally by

$$\begin{pmatrix} F_x(\varphi_r) \\ F_y(\varphi_r) \\ T_z(\varphi_r) \end{pmatrix} = \begin{pmatrix} \mathbf{i}_s^T & \mathbf{O}_{1\times m} & \mathbf{O}_{1\times m} \\ \mathbf{O}_{1\times m} & \mathbf{i}_s^T & \mathbf{O}_{1\times m} \\ \mathbf{O}_{1\times m} & \mathbf{O}_{1\times m} & \mathbf{i}_s^T \end{pmatrix} \mathbf{T}_Q(\varphi_r)\mathbf{i}_s + \mathbf{T}_L(\varphi_r)\mathbf{i}_s + \mathbf{T}_N(\varphi_r), \tag{1}$$

where $\mathbf{i}_s$ represents the stator coil current vector composed of the m phase currents, $\mathbf{O}_{k\times l}$ specifies a zero matrix of the subscripted order and φ_r describes the rotor angle. Nonlinear effects (like saturation or demagnetization) are neglected in this modeling.

However, in (1) there is a term with a quadratic ($\mathbf{T}_Q(\varphi_r)$), a linear ($\mathbf{T}_L(\varphi_r)$) and no ($\mathbf{T}_N(\varphi_r)$) dependency on the stator current vector. $\mathbf{T}_Q(\varphi_r)$ represents the reluctance forces and torque due to the stator currents and $\mathbf{T}_N(\varphi_r)$ the reluctance forces and torque due to the permanent magnets. Normally $\mathbf{T}_N(\varphi_r)$ is small and can be neglected or compensated. A Taylor series development of first order at zero phase currents leaves only the linear current dependency of the bearing forces and motor torque

$$\begin{pmatrix} F_x(\varphi_r) \\ F_y(\varphi_r) \\ T_z(\varphi_r) \end{pmatrix} = \mathbf{T}_L(\varphi_r)\mathbf{i}_s. \tag{2}$$

This linearization is only valid, when the forces and torque created by the stator currents even under consideration of the $\mathbf{T}_Q(\varphi_r)$-term remain approximately linear. That is only the case when the quadratic force and torque component is much smaller than the linear term. For surface mounted rotor magnets but also for a lot of buried and inset rotor permanent magnets this assumption holds true.

To obtain the entries of the matrix $\mathbf{T}_L(\varphi_r)$ one phase has to be energized with a constant magnetomotive force. The linear motor torque and the resulting linear forces in x_r- and y_r-direction, which are exerted on the rotor over a full electric period, represent the data of one column in the matrix (referring to the chosen stator current). For a symmetric stator arrangement and a winding system, where the neighboring phases are shifted by a mechanical angle of

$$\tau = \frac{2\pi}{m}, \tag{3}$$

the entries of $\mathbf{T}_L(\varphi_r)$ are not independent from each other. This precondition is very often fulfilled. Thus, the whole matrix can be computed from one column by the use of two coordinate transformations. The first considers the geometric displacement of the phases, the second takes the different rotor angle positions with reference to each phase into account. The m phases representation of this matrix

$$\mathbf{T}_L(\varphi_r) = \begin{pmatrix} T_{11}(\varphi_r) & T_{21}(\varphi_r) & T_{31}(\varphi_r) & \cdots & T_{m1}(\varphi_r) \\ T_{12}(\varphi_r) & T_{22}(\varphi_r) & T_{32}(\varphi_r) & \cdots & T_{m2}(\varphi_r) \\ T_{13}(\varphi_r) & T_{23}(\varphi_r) & T_{33}(\varphi_r) & \cdots & T_{m3}(\varphi_r) \end{pmatrix} \tag{4}$$

can be computed from the first row for all $n \in \mathbb{N} \,|\, 1 \le n \le m$ by

$$\begin{pmatrix} T_{n1}(\varphi_r) \\ T_{n2}(\varphi_r) \\ T_{n3}(\varphi_r) \end{pmatrix} = \begin{pmatrix} \cos(\tau(n-1)) & -\sin(\tau(n-1)) & 0 \\ \sin(\tau(n-1)) & \cos(\tau(n-1)) & 0 \\ 0 & 0 & 1 \end{pmatrix} \begin{pmatrix} T_{11}(\varphi_r - \tau p_z(n-1)) \\ T_{12}(\varphi_r - \tau p_z(n-1)) \\ T_{13}(\varphi_r - \tau p_z(n-1)) \end{pmatrix}. \tag{5}$$

It is assumed that all neighbouring phases are located in ascending order over the circumference of the stator. Using (5) to compute all entries of $\mathbf{T}_L(\varphi_r)$ from one column reduces the needed computational time for finite element simulations drastically. However, it is important to consider that a computation of forces and torque by $\mathbf{T}_L(\varphi_r)$ will only lead to valid results for negligible influence of the nonlinear effects and of $\mathbf{T}_Q(\varphi_r)$. For reluctance rotors, especially the latter condition is not necessarily true (as it is nearly always in permanent magnet excited rotors) and must be checked carefully.

3.2 Decoupling of Force and Torque

The matrix $\mathbf{T}_L(\varphi_r)$ gives the relation of the bearing forces and the motor torque generated by the energized stator coils. For the control scheme, the inverse relation is needed. To allow an inversion,

$$\mathbf{T}_\mathbf{L}(\varphi_r)\mathbf{K}_\mathbf{L}(\varphi_r) = \mathbf{I}_3 \tag{6}$$

has to be true. By the help of $\mathbf{K}_L(\varphi_r)$, the currents can be computed, which have to be impressed into the coils for creating a defined bearing force and motor torque, by

$$\mathbf{i}_s = \mathbf{K}_\mathbf{L}(\varphi_r) \begin{pmatrix} F_x(\varphi_r) \\ F_y(\varphi_r) \\ T_z(\varphi_r) \end{pmatrix}. \tag{7}$$

A possible solution for this problem is given by the pseudo-inverse (Moore-Penrose-inverse) [14] minimizing the copper losses and yields

$$\mathbf{K}_\mathbf{L}(\varphi_r) = \mathbf{T}_\mathbf{L}(\varphi_r)^T \left(\mathbf{T}_\mathbf{L}(\varphi_r) \mathbf{T}_\mathbf{L}(\varphi_r)^T \right)^{-1}. \tag{8}$$

3.3 Performance Parameters

To judge the operational behavior of the bearingless slice reluctance motor performance parameters are specified. For this reason a force factor k_f and a torque factor k_t are defined. The force factor represents the ratio between the maximum phase force and the minimum overall force of the whole motor (contributed properly by all m phases) for a maximum allowed current linkage per coil. The torque factor describes the same ratio for the motor torque. When $k_{L,ij}(\varphi_r)$ stands for the entry of the matrix $\mathbf{K}_L(\varphi_r)$ in column i and row j, the referring force factor is defined by

$$k_f = \frac{F_{overall,min}}{F_{phase,max}} = \min_{i=1,2}\left(\frac{1}{\max\limits_{j,\varphi_r} \left| k_{L,ij}(\varphi_r) \right|} \right) \tag{9}$$

and the torque factor yields

$$k_t = \frac{T_{overall,min}}{T_{phase,max}} = \frac{1}{\max\limits_{j,\varphi_r} \left| k_{L,3j}(\varphi_r) \right|} \tag{10}$$

accordingly. It is obvious that the factors must be smaller than or equal to m, the total phase number. Referring to common drives with mechanical bearings and ideal sinusoidal induced voltage, the torque factor is normally $m/2$.

4 Homopolar Bearingless Reluctance Slice Motor

4.1 Principle of Operation

In homopolar bearingless reluctance slice motors the force generation works similar to permanent magnet biased active magnetic bearings. The bias flux is strengthened or weakened by the electromagnetic flux created by one stator coil, leading to a radial pull or push force towards the energized concentric stator coil [15]. Due to the reluctance of the rotor the resulting force is not constant over the rotor angle. Normally, there is only a negligible force component in tangential direction of the energized stator tooth.

The variation in the permanent magnet bias flux over the rotor angle and its dependency on the reluctance lead to a variation in the flux linkage of the stator coils and, therefore, to an induced voltage and torque generation. In a first approximation this torque characteristic can be modeled sinusoidally. Figure 5 depicts the announced force and torque behavior of one phase over the rotor angle for a constant current linkage.

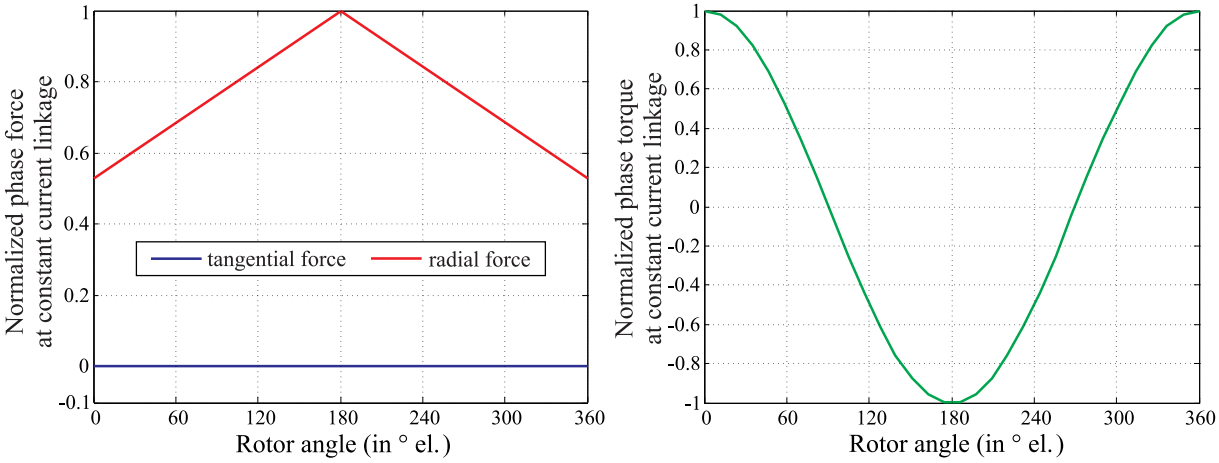

Figure 5: Bearing force and torque characteristic of one phase of a homopolar reluctance slice motor at constant current linkage. The force is separated in radial and tangential direction with reference to the energized coil.

It can be seen that the curves have been normalized. They are related to their maximum value and are thus within a range of -1 and 1.

4.2 Performance Comparison

The force and torque curves in Fig. 5 are represented by the entries of one column of the matrix $\mathbf{T}_L(\varphi_r)$. Using (5), the overall matrix can be computed. Thus, also $\mathrm{K}_L(\varphi_r)$ and furthermore also the performance parameters k_f and k_t can be derived. It is obvious that they are all dependant on the number of rotor pole pairs p_z and the number of stator teeth, which is equal to the number of motor phases m in the considered case. For reluctance motors the number of pole pairs is defined as the number of inductivity periods over one full mechanical rotation.

Table 1 contains the performance parameters for four to nine phase machines with rotor pole pairs from two to eight. It is clearly visible that some combinations (featuring higher performance factors) lead to superior machines. A torque factor k_t of zero indicates single phase characteristic of the drive system, which can be acceptable for some applications. The motors, whose performance factors are plotted in faded numbers, refer to unlikely stator phase to rotor pole pair combinations due to geometrical restrictions.

	p_z=2	p_z=3	p_z=4	p_z=5	p_z=6	p_z=7	p_z=8
m=4	k_f=1.0 k_t=0.0	k_f=0.4 k_t=0.4	k_f=1.0 k_t=0.0	k_f=0.4 k_t=0.4	k_f=1.0 k_t=0.0	k_f=0.4 k_t=0.4	k_f=1.0 k_t=0.0
m=5	k_f=1.6 k_t=2.1	k_f=1.6 k_t=2.1	k_f=0.4 k_t=0.5	k_f=1.3 k_t=0.0	k_f=0.4 k_t=0.5	k_f=1.6 k_t=2.1	k_f=1.6 k_t=2.1
m=6	k_f=2.1 k_t=2.9	k_f=2.1 k_t=0	k_f=2.1 k_t=2.9	k_f=0.5 k_t=0.6	k_f=1.6 k_t=0.0	k_f=0.5 k_t=0.6	k_f=2.1 k_t=2.9
m=7	k_f=2.5 k_t=3.5	k_f=2.3 k_t=3.2	k_f=2.3 k_t=3.2	k_f=2.5 k_t=3.5	k_f=0.5 k_t=0.6	k_f=1.8 k_t=0.0	k_f=0.5 k_t=0.6
m=8	k_f=2.9 k_t=4.0	k_f=2.5 k_t=4.0	k_f=2.5 k_t=0.0	k_f=2.5 k_t=4.0	k_f=3.0 k_t=4.0	k_f=0.6 k_t=0.8	k_f=2.1 k_t=0.0
m=9	k_f=3.2 k_t=4.5	k_f=3.0 k_t=4.3	k_f=3.0 k_t=4.0	k_f=3.0 k_t=4.0	k_f=3.0 k_t=4.3	k_f=3.2 k_t=4.5	k_f=0.7 k_t=0.8

Table 1: Performance parameters of the homopolar bearingless reluctance slice motor

When taking a closer look at Table 1 it becomes clear that a choice of $m = p_z \pm 2$ for $m > 4$ will lead to favorable designs concerning high force and torque factors. These designs are marked by the grey background in the chart.

5 Heteropolar Bearingless Reluctance Slice Motor

Concerning the heteropolar bearingless reluctance slice motors, a lot of different stator variants are imaginable [12]. Unfortunately, they do not feature a unique bearing force and torque characteristic. The two designs, depicted in Fig. 3, show a very strong reluctance term due to the currents, which leads to the fact, that the linearization (2) is not a valid description.

The next sections concern (and hold true) for the bearingless reluctance drives visible in Fig. 2. They feature nearly the same approximately linear operational characteristic. So (2) is an applicable mathematical description.

5.1 Principle of Operation

The linear force and torque characteristic of the bearingless reluctance drives featuring two permanent magnetic poles on one stator tooth are illustrated in Fig. 6. The torque characteristic is approximated by a sinusoidal curve. The force orbit is ellipsoidal, which is very common in permanent magnet excited bearingless slice motors [16]. Unique is the deflection of the orbit in tangential direction (with reference to the energized stator coil). This behavior results from the fact that each stator tooth features a permanent magnetic pole pair. The electromagnetic flux of one coil therefore weakens and strengthens the permanent magnetic poles of one stator tooth simultaneously, resulting in a radial and tangential force.

The curves of Fig. 6 have been normalized and are thus related to their maximum value.

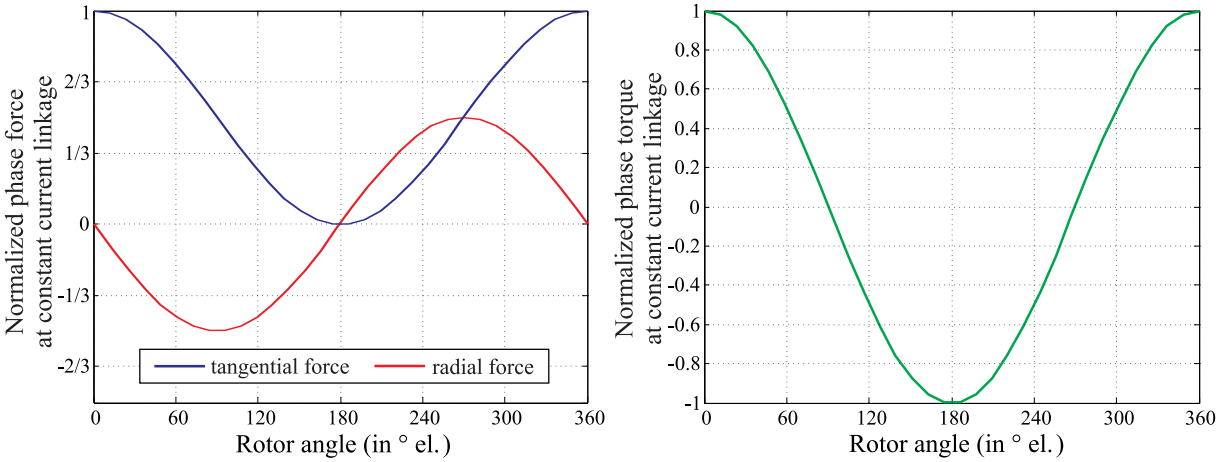

Figure 6: Bearing force and torque characteristic of one phase of the considered heteropolar reluctance slice motors at constant current linkage.

5.2 Performance Comparison

With the help of the bearing force and torque characteristic the performance parameters can be computed for different rotor pole pair and stator phase combinations. Table 2 contains all the performance parameters for four to nine stator phases combined with rotor pole pairs from two to nine.

	p_z=2	p_z=3	p_z=4	p_z=5	p_z=6	p_z=7	p_z=8	p_z=9
m=4	k_f=0.0 k_t=0.0	k_f=0.0 k_t=0.0	k_f=0.0 k_t=0.0	k_f=1.0 k_t=1.3	k_f=0.0 k_t=0.0	k_f=0.0 k_t=0.0	k_f=0.0 k_t=0.0	k_f=1.0 k_t=1.3
m=5	k_f=0.0 k_t=0.0	k_f=1.1 k_t=1.2	k_f=1.1 k_t=1.2	k_f=0.0 k_t=0.0	k_f=1.1 k_t=1.7	k_f=0.0 k_t=0.0	k_f=1.1 k_t=1.2	k_f=1.1 k_t=1.2
m=6	k_f=0.0 k_t=0.0	k_f=1.5 k_t=0.0	k_f=1.4 k_t=3.0	k_f=1.3 k_t=1.5	k_f=0.0 k_t=0.0	k_f=1.4 k_t=2.0	k_f=0.0 k_t=0.0	k_f=1.0 k_t=0.0
m=7	k_f=0.0 k_t=0.0	k_f=1.7 k_t=3.5	k_f=1.5 k_t=1.7	k_f=1.7 k_t=3.5	k_f=1.5 k_t=1.7	k_f=0.0 k_t=0.0	k_f=1.5 k_t=2.3	k_f=0.0 k_t=0.0
m=8	k_f=0.0 k_t=0.0	k_f=2.0 k_t=4.0	k_f=2.0 k_t=0.0	k_f=1.9 k_t=4.0	k_f=2.0 k_t=4.0	k_f=1.8 k_t=2.0	k_f=0.0 k_t=0.0	k_f=1.8 k_t=2.7
m=9	k_f=0.0 k_t=0.0	k_f=2.3 k_t=4.5	k_f=2.3 k_t=4.5	k_f=2.0 k_t=2.3	k_f=2.3 k_t=4.5	k_f=2.3 k_t=4.5	k_f=2.0 k_t=2.3	k_f=0.0 k_t=0.0

Table 2: Performance parameters of the considered heteropolar bearingless reluctance slice motor.

Designs that fulfill $m = p_z - 1$ or $m = p_z + 2$ with $m > 5$ will result in promising designs concerning high force and torque generation capability with respect to one phase. The most advantageous designs are indicated by a grey background in the table.

It is visible in Table 2 that there are combinations featuring single phase characteristic in the torque and also in the bearing force. All combinations, that possess force factors of zero, are not able to work as bearingless motor properly and are marked with red backgrounds. Due to geometrical restrictions some motor combinations are unfavorable, their performance factors are faded.

Comparing Table 1 and 2 it becomes obvious, that the force factors of the favorable homopolar bearingless motors are higher than for advantageous heteropolar motor types. In contrast to that, the torque factors are in a comparable range.

Considering four phase machines, the heteropolar bearingless slice motor with five rotor pole pairs features an outstanding performance in both force and torque. So far, all bearingless motors (with permanent magnet excited rotors) with only four concentric coils in the stator have possessed single phase torque characteristics. This is not the case with the considered heteropolar bearingless reluctance slice motor with p_z equal to five.

5.3 Prototype Motor

With the help of Table 2, a prototype design was chosen. It was stated before that a heteropolar bearingless reluctance slice motor with only four stator teeth (and therefore only four coils) in combination with a ferromagnetic rotor with five salient poles looks very promising. Figure 7 shows the selected interior stator and exterior rotor design. The bias air gap flux is generated from permanent magnets that are mounted on the surface of the stator teeth. Two magnets with opposing radial magnetization direction are placed on each stator tooth.

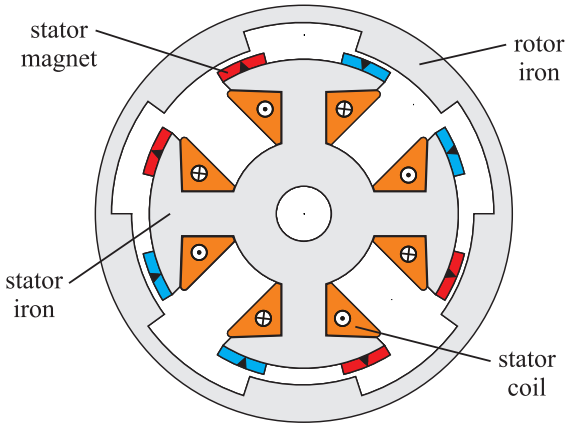

Figure 7: Drawing of the optimized heteropolar bearingless slice motor with external rotor.

The various geometric design parameters were optimized with the help of finite element simulations embedded in a multi-criteria genetic algorithm. Optimization criteria were the cogging torque, the permanent magnetic reluctance forces, the motor torque and the bearing forces [17].

The setup of the optimized bearingless motor prototype is depicted in Fig. 8. The stator and rotor yoke were wire cut from V270-35A laminated steel stacks. The four concentric coils were manually wound around the stator teeth and connected in star. The permanent magnets feature a remanence flux density of 1.2 T and were easily adjusted and fixed on the surface of the stator iron. In-between the two magnets that are located on the same stator pole, a teflon block was placed acting as auxiliary bearing. The reluctance rotor was embedded in an aluminum housing to allow the use of eddy current sensors, which are located inside the stator slots. Additionally, an acrylic glass hood was mounted on the rotor. It holds a permanent magnet, which enables the detection of the angular rotor position by an integrated Hall sensor circuit.

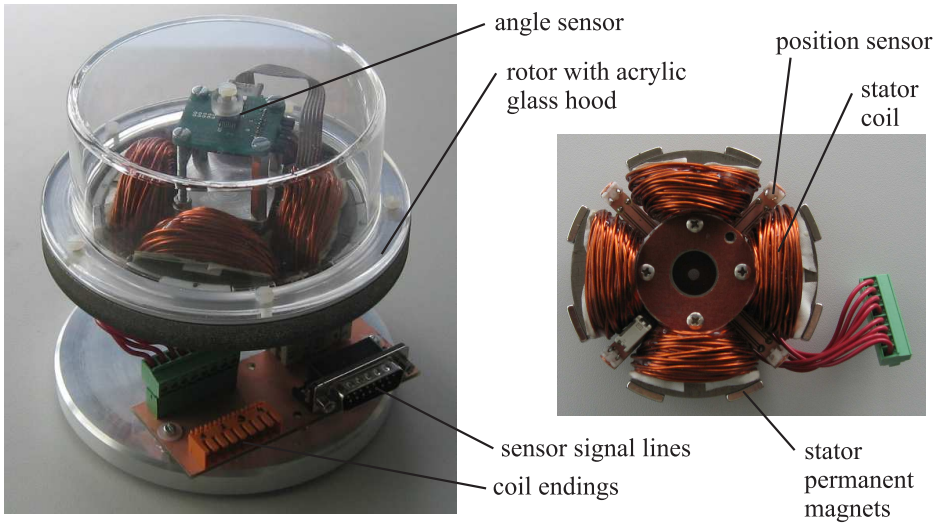

Figure 8: Picture of the manufactured prototype.

A proper control scheme or stabilizing the rotor position and controlling the torque is given in [18]. It makes use of the matrix $\mathbf{K}_L(\varphi_r)$ and is based on nonlinear feedback control in order to linearize the plant and allow the use of well known linear and time invariant control design methods. Concerning the realization and implementation of the control scheme in hardware, a 16 bit fixed point digital signal processor was employed. The software was written in C-code to alleviate modifications or extensions. The controller is capable to perform up to 150 MIPS, allowing a sampling time of 100 µsec. The controller system is well-integrated in a power electronic circuit, which operates with a supply voltage of 70 V DC, featuring four half bridges controlled with a 30 kHz PWM signal and is capable of delivering a maximum output current of 10 A per channel.

5.4 Measurements

To confirm the results obtained by the simulation, measurements have been carried out with the prototype drive. For this purpose, the bearingless reluctance slice motor was fixed on a test bench, which is equipped with a load cell for measuring the bearing forces. One coil was energized constantly exerting a current linkage of 1000 Aturns. The resulting bearing force acting on the rotor is visible in the left illustration of Fig. 9 for certain rotational angles. The measured orbit points are compared with the expected shape derived from the finite element simulations. The difference between the two dimensional finite element simulations and the measurement is relatively small and originates in the axial leakage flux and material uncertainties. As expected, the orbit is shifted out of the origin in a way that is also shown in Fig. 6.

Additionally, the torque generation capability was examined. This was achieved by measuring the induced voltage of a stator coil, when the rotor was mechanically suspended and driven externally at constant speed by a direct current machine. Dividing the measured induced voltage value by the rotational speed delivers the torque per current ratio. As visualized in the right-hand side of Fig. 9 the simulated and measured curves are of the same shape and therefore show a very good correlation. The error is again within a range of 15%.

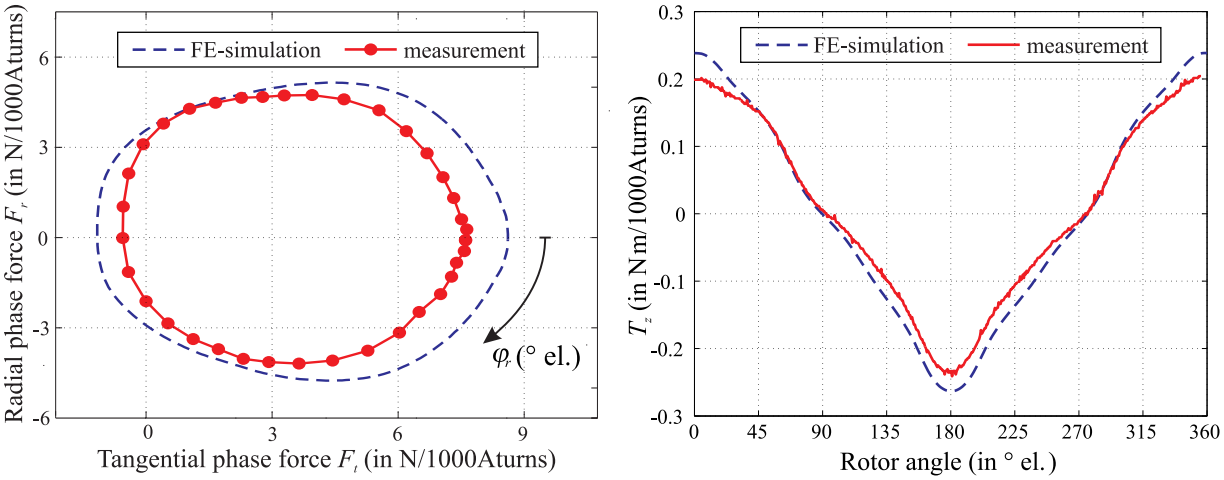

Figure 9: Comparision of measurement and simulation results of the phase force and torque.

6 Conclusion

In this paper a new type of bearingless slice motor, the bearingless reluctance slice motor, is introduced. The mechanical composition of this bearingless motor is relatively simple. The rotor carries no permanent magnets and is therefore cheap and robust. Several possible design variants are considered. A distinction between hompolar and heteropolar bearingless reluctance motors is made. Performance factors are defined and computed for different machine types to evaluate the different designs.

A prototype bearingless reluctance slice motor with external rotor design was designed, optimized and put into operation. It features only four stator poles with concentrated windings. Due to its unique characteristics concerning the bearing force generation, the single phase torque behavior, which is typical for comparable bearingless slice motors with permanent magnets in the rotor, is avoided. First measurements approve the theoretical considerations

and finite element simulation results. The novel bearingless drive shows the expected behavior in both motor and bearing performance.

Acknowledgement

The presented research work has been supported by the ACCM GmbH[1], which is part of the COMET/K program of the Federal Ministry of Transport, Innovation and Technology and the Federal Ministry of Economics and Labor in Austria. The authors thank all involved partners for their support in making this work possible.

References

[1] A. O. Salazar, A. Chiba, T. Fukao, "A Review of Developments in Bearingless Motors", Proc. 7th Int. Symposium on Magnetic Bearings (ISMB7), pp. 335-340, 2000

[2] M. Ooshima, S. Kobayashi, H. Tanaka, "Magnetic suspension performance of a bearingless motor/generator for flywheel energy storage systems", Proc. 2010 IEEE Power and Energy Society General Meeting, pp. 1-4, 2010

[3] H. Mitterhofer, W. Amrhein, "Motion Control Strategy and Operational Behaviour of a High Speed Bearingless Disc Drive", Proc. 2012 Power Electronics, Machines and Drives Conf. (PEMD2012), Bristol (UK), 2012

[4] M. Neff, N. Barletta, R. Schöb, "Bearingless centrifugal pump for highly pure chemicals," Proc. 8th Int. Symp. on Magnetic Bearing (ISMB8), pp. 283–288, 2002

[5] R. Schöb, N. Barletta, "Principle and application of a bearingless slice motor", Proc. 5th Int. Symposium on Magnetic Bearings (ISMB5), Kanazawa (Japan), p. 313f, 1996

[6] S. Silber, W. Amrhein, P. Bosch, R. Schöb, N. Barletta, "Design aspects of bearingless slice motors" IEEE/ASME Trans. on Mechatronics, vol. 10, no. 6, pp. 611- 617, Dec. 2005

[7] P. Karutz, T. Nussbaumer, J. W. Kolar, "Magnetically levitated slice motors - an overview", Proc. 1st IEEE Energy Conversion Congress and Exposition (ECCE2009), San Jose (USA), pp. 1494-1501, 2009

[8] C. R. Morrison, M. W. Siebert, E. J. Ho, "Electromagnetic Forces in a Hybrid Magnetic-Bearing Switched-Reluctance Motor", IEEE Trans. on Magnetics, vol. 44, no. 12, pp. 4626-4638, Dec. 2008

[9] M. Takemoto, H. Suzuki, A. Chiba, T. Fukao, M. A. Rahman, "Improved analysis of a bearingless switched reluctance motor", IEEE Trans. on Industry Applications, vol. 37, no. 1, pp. 26-34, Jan/Feb 2001

[10] Y. Yan, D. Zhiquan, Y. Gang, C. Xin, Z. Qianying, "A Control Strategy for Bearingless Switched-Reluctance Motors", IEEE Transactions on Power Electronics, vol. 25, no. 11, pp. 2807-2819, Nov. 2010

[11] W. Hua, Z. Q. Zhu, M. Cheng, Y. Pang, D. Howe, "Comparison of flux-switching and doubly-salient permanent magnet brushless machines", Proc. 8th Int. Conf. on Electrical Machines and Systems (ICEMS8), vol. 1, pp. 165-170, 2005

[12] W. Amrhein, H. Grabner, W. Gruber, S. Silber, "Elektrische Maschine mit einem magnetisch gelagerten Reluktanzläufer", Austrian Patent Application A803, 2011

[13] W. Amrhein, S. Silber, K. Nenninger, "Levitation forces in bearingless permanent magnet motors", IEEE Trans. on Magnetics, vol. 35, no. 5, part 2, pp 4052-4054, 1999

[14] S. Silber, W. Amrhein, "Power Optimal Current Control Scheme for Bearingless PM Motors", Proc. 7th Int. Symp. on Magnetic Bearings (ISMB7), pp. 401-306, 2000

[15] M. Reisinger, W. Amrhein, S. Silber, "A Novel Design of a Magnetic Bearing Biased with Permanent Magnets", Proc. 2003 Int. Exh. and Conf. for Power Conversion and Intelligent Motion (PCIM2003), Nurnberg, 2003

[16] W. Gruber, S. Silber, W. Amrhein, T. Nussbaumer, "Design variants of the bearingless segment motor", Proc. 2010 Int. Symp. on Power Electronics Electrical Drives Automation and Motion (SPEEDAM2010), pp. 1448 -1453, 2010

[17] W. Gruber, W Briewasser, W. Amrhein, "Novel bearingless slice motor design with four concentrated coils featuring a unique operational behavior", Proc. 14th European Conference on Power Electronics and Applications (EPE'11), Birmingham (UK), 2011

[18] H. Grabner, W. Amrhein, S. Silber, W. Gruber, "Nonlinear Feedback Control of a Bearingless Brushless DC Motor", IEEE/ASME Trans. on Mechatronics, vol. 15, no. 1, pp. 40-47, Feb. 2010

[1] Austrian Center of Competence in Mechatronics, http://accm.co.at